



3D modelling of edge parallel flow asymmetries

P. Tamain^{a,b,*}, Ph. Ghendrih^a, E. Tsitrone^a, Y. Sarazin^a, X. Garbet^a, V. Grandgirard^a,
J. Gunn^a, E. Serre^c, G. Ciraolo^c, G. Chiavassa^c

^aAssociation Euratom-CEA, CEA Cadarache, F-13108 St. Paul-lez-Durance, France

^bEURATOM/UKAEA Fusion Association, Culham Science Centre, Abingdon, D3/G22, Oxon OX14 3DB, UK

^cMSNM-GP-UMR 6181, CNRS/Aix-Marseille-Université, La Jetée-Technopôle de Château-Gombert, 38 rue Frédéric Joliot-Curie, 13451 Marseille Cedex 20, France

ARTICLE INFO

PACS:

52.55.Fa

52.30.Ex

52.25.Fi

52.35.Ra

ABSTRACT

The issue of parallel flows asymmetries in the edge plasma is tackled with a new first principle transport and turbulence code. *TOKAM-3D* is a 3D full-torus fluid code that can be used both in diffusive and turbulent regimes and covers either exclusively closed flux surfaces or both open and closed field lines in limiter geometry. Two independent mechanisms susceptible to lead to large amplitude asymmetric parallel flows are evidenced. Global ExB drifts coupled with the presence of the limiter break the poloidal symmetry and can generate large amplitude parallel flows even with poloidally uniform transport coefficients. On the other hand, turbulent transport in the edge exhibits a strong ballooning of the radial particle flux generating an up-down $m = 1$, $n = 0$ structure on the parallel velocity. The combination of both mechanisms in complete simulations leads to a poloidal and radial distribution of the parallel velocity comparable to experimental results.

© 2009 Elsevier B.V. All rights reserved.

1. Introduction

Momentum transport in the edge plasma of tokamaks has recently appeared as a major issue in fusion research with the observation on all machines of a so-called spontaneous rotation of the plasma in the poloidal and toroidal directions [1].

One of the most striking experimental evidence for momentum transport is the issue of edge parallel flow poloidal asymmetries. Indeed, measurements performed in the Scrape Off Layer (SOL) of different machines at different poloidal locations exhibit a common asymmetric behaviour of the poloidal distribution of the parallel velocity [2]. The effect is not restricted to diverted tokamaks; it is also seen in Tore Supra, which employs a toroidal belt limiter to define the LCFS. In particular, a parallel mach number equal to $M \approx 0.5$ ($M = u_{\parallel}/c_s$ is the ionic parallel velocity normalised by the acoustic velocity $c_s = \sqrt{(T_e + T_i)/m_i}$) is measured at the top of the machine, where symmetry considerations suggest that the stagnation point $M \sim 0$ should be found [3].

Modelling of this phenomenon by transport codes has been attempted and has demonstrated a possible role of large scale drifts [4,5]. However, experimental amplitudes can only be reached by assuming a strong ballooning of the radial transport, with an anomalous diffusion coefficient 200 times higher on the Low Field Side (LFS) compared to the High Field Side (HFS) [6].

In this paper, we address the issue of edge parallel flow asymmetries using the new edge transport and turbulence code *TOKAM-3D* [7,8]. This code solves fluid-drift equations without scale separation in 3D full-torus geometry and is therefore able to handle coherently small turbulent structures as well as global drifts. Furthermore, the simulated region can cover both closed and open flux surfaces. These features make it particularly adapted to tackling these issues.

2. The TOKAM-3D code

TOKAM-3D is a first principle transport and turbulence code for the edge plasma. A fully detailed description is given in Refs. [7,8]. It solves balance equation for the density N , the electrostatic potential Φ , the parallel current J_{\parallel} and the parallel velocity M , which is normalized by the acoustic velocity c_s , following the same kind of approach as Ref. [9]. The plasma is assumed isothermal with $T_e = T_i$. The modelled region is a toroidal ring of plasma between minor radii r_{\min} and r_{\max} (Fig. 1), where $r_{\min} < a$ and a is the minor radius at the Last Closed Flux Surface (LCFS). If $r_{\max} > a$, it covers both closed and open flux surfaces in limiter configuration, the limiter occupying an angular sector Δ_{lim} at the bottom of the machine where it imposes Bohm boundary conditions. Otherwise, $r_{\max} = a$ and the code treats exclusively outermost closed flux surfaces up to the LCFS. We will designate these two variants as the ‘edge’ and ‘edge/SOL’ versions. In both cases, the system is driven by a poloidally symmetric volumetric particle source located close to the inner boundary $r = r_{\min}$.

* Corresponding author. Address: EURATOM/UKAEA Fusion Association, Culham Science Centre, Abingdon, D3/G22, Oxon OX14 3DB, UK.

E-mail address: patrick.tamain@ukaea.org.uk (P. Tamain).

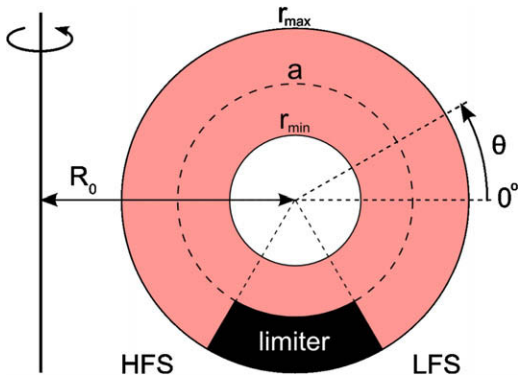


Fig. 1. Poloidal cross-section of the geometry of the TOKAM-3D code. The filled area corresponds to the simulated region in the edge/SOL version.

TOKAM-3D also offers some flexibility in the range of transport regimes it can address. By simply acting on the diffusion coefficients D_{\perp} (set equal for particle, momentum and current diffusion), it can be used as a global diffusive transport code modelling exclusively large scale structures (typically $D_{\perp} > 0.1$) or as a full-torus turbulence code but still handling coherently global flows (typically $D_{\perp} < 0.1$). These two extreme regimes will be designated as ‘laminar’ and ‘turbulent’.

3. Effect of large scale drifts

So as to study the possible role of large scale drifts on the development of parallel flow asymmetries, without having to deal with any effect linked to intrinsic properties of turbulent transport, we consider a simulation run with the edge/SOL version in the laminar regime with homogeneous diffusion coefficients: $a = 100$, $a - r_{\min} = 50$, $r_{\max} - a = 50$, $R_0/a = 3.4$ and $D_{\perp} = 0.2$ (distances are normalized to the ion gyro-radius ρ_L and time to the inverse of the cyclotron frequency).

The results show the development of an asymmetric poloidal structure in the parallel velocity in the SOL (Fig. 2). The radial profile of the Mach number at 3 different poloidal locations and the poloidal profile just outside the LCFS are also given. The structure is mainly located on the SOL side of the LCFS, with a non-zero Mach number around $M \approx 0.25$ observed at the top of the machine at $r - a = 20$. The $M > 0$ area extends on the LFS towards the limiter further than the equatorial plane.

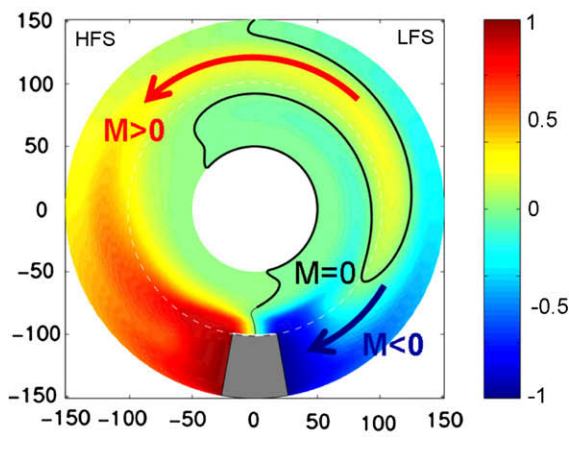


Fig. 2. Parallel Mach number in the laminar regime. Left: poloidal cross-section with $M = 0$ iso-contour. Right: radial profiles at the top of the machine and in the equatorial plane.

An explanation for the development of this asymmetry is found in the existence of a global poloidal ExB rotation induced by the development of a radial potential profile determined by current balance. This rotation of the plasma associated with the obstacle that constitutes the limiter leads to a density accumulation on the LFS of the limiter which feeds back parallel flows through the parallel pressure gradient. An additional contribution from the Pfirsch–Schlüter flow and from the poloidal compression of the ExB rotation can be observed in the outboard mid-plane with an amplitude $M \approx 0.1$. However, those effects do not contribute to the Mach number at the top of the machine.

4. Effect of intrinsic properties of turbulent transport

We now switch to the other mechanism suggested to be likely to generate parallel flows: the probable ballooning of the radial turbulent transport. In order to do so without having to deal with large scale effects linked to the presence of the limiter, we use the edge version of TOKAM-3D and place ourselves in the turbulent regime: $a = 200$, $a - r_{\min} = 80$, $r_{\max} = a$, $R_0/a = 3.4$ and $D_{\perp} = 0.02$ (spatially constant).

Fig. 3 shows a poloidal iso-contour plot of the parallel velocity in the established non-linear turbulent regime. Turbulence is characterized by small scale fluctuating structures strongly aligned

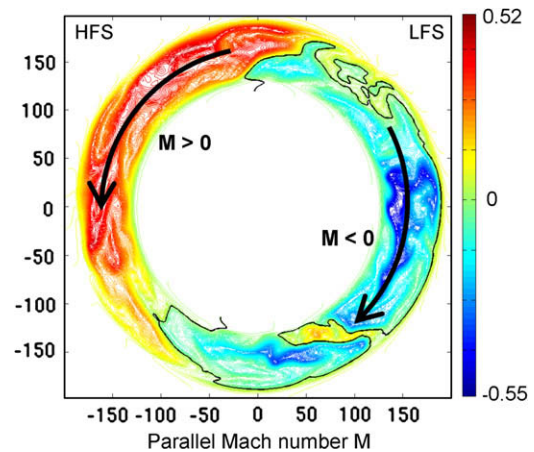


Fig. 3. Poloidal cross-section of the parallel velocity in the turbulent regime (instantaneous snapshot). The black line is the $M = 0$ iso-contour.

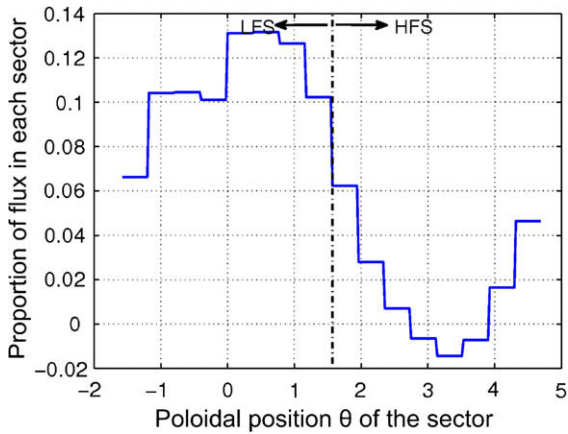


Fig. 4. Proportion of the total radial turbulent flux transported in each angular sector Σ_i as a function of the poloidal position.

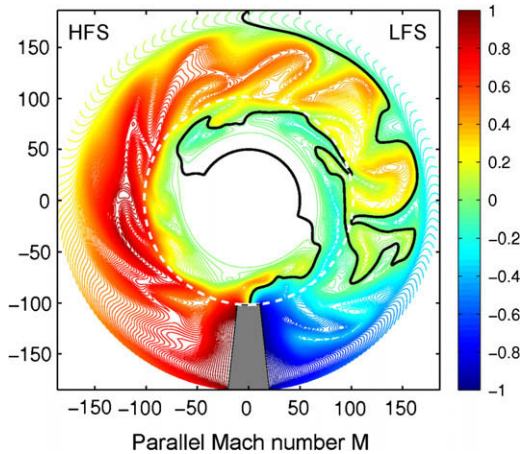


Fig. 5. Poloidal cross-section (instantaneous snapshot) of the parallel velocity after the turbulent regime has been reached with the edge/SOL version of TOKAM-3D. The black line is the $M = 0$ iso-contour.

along the magnetic field. However, the main noticeable feature is the existence of an $(m = 1, n = 0)$ structure with an amplitude $M \approx 0.4$ – 0.5 .

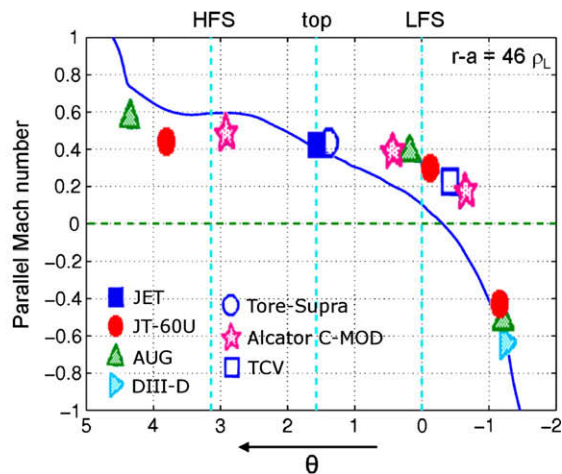
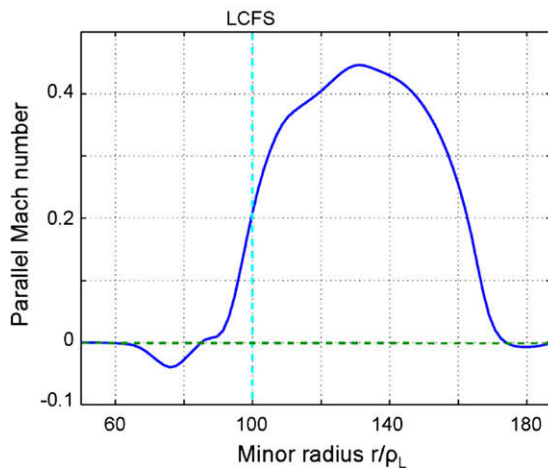


Fig. 6. Toroidally averaged profiles of the parallel Mach number after the turbulent regime has been reached with the edge/SOL version of TOKAM-3D. Left: radial profile at the top of the machine. Right: poloidal profile at $r - a = 46 \rho_L$; the symbols correspond to multi-machine experimental results compiled in [2].

To explain this behaviour, it is necessary to study the poloidal distribution of the turbulent transport. Let us divide the poloidal direction in 16 equal angular sectors Σ_i and compute the proportion $P_{r_i}^{\Sigma_i}$ of the total particle flux flowing radially through each sector. The poloidal distribution of $P_{r_i}^{\Sigma_i}$ is given on Fig. 4. The LFS is characterized by a homogeneous flux of 10–12% per sector while the flux drops on the HFS down to slightly negative values at the inboard equatorial plane. The LFS is found to carry 90% of the total flux. This result is in good agreement with the estimation proposed in Ref. [3], although no similar sharp peaking around the equatorial plane is observed. Note that since the diffusion coefficients are set spatially constant, the poloidal inhomogeneity of the radial transport is consistently driven by the interplay between turbulence and curvature.

The main consequence of the ballooning of the radial flux is an inhomogeneous poloidal distribution of the averaged density. Parallel flows are then generated by parallel pressure gradients to counterbalance this mechanism. One may, however, notice that the $m = 1$ structure shown on Fig. 3 is not aligned with the equatorial plane. This is linked to the existence of a negative radial electric field that generates a poloidal ExB drift (anti-clockwise on Fig. 3), which, in turn, advects parallel momentum and tilts the parallel velocity structure.

5. Combination of both mechanisms

In the SOL of tokamaks, both previous effects should overlap. To obtain a fully consistent insight on the physics at stake, we consider a case run in the turbulent regime with the edge/SOL version of the code: $a = 100$, $a - r_{\min} = 50$, $r_{\max} - a = 83$, $R_0/a = 3.4$ and $D_{\perp} = 0.08$.

Fig. 5 shows a poloidal cross-section of the parallel velocity. As expected, turbulent structures are localized mainly on the LFS and overlap with the laminar asymmetric structure described in Section 2. The Mach number at the top of the machine is found equal to $M \approx 0.4$ – 0.5 , which is in good agreement with experimental amplitudes [2].

A more advanced comparison with experimental data can be obtained by looking at the toroidally averaged poloidal distribution of the parallel Mach number in the middle of the SOL (Fig. 6). The curve obtained in our simulation is qualitatively very similar to multi-machine data compiled in Ref. [2]. Some difference can be noticed on the LFS where the rise of the parallel velocity from $M = -1$ at the limiter plate to $M \approx 0.4$ at the top is not as steep

as experimental observations suggest. This discrepancy might be linked to the recycling source (which is not included in our simulation) and the fact that, for mesh and computation time reasons, the diffusion coefficients used here are higher than the classical ones which should be used to have a proper description of turbulent transport.

An interesting feature can be noticed on the radial profile of the parallel velocity at the top of the machine, also shown in Fig. 6. Compared to the laminar profile (Fig. 2), a deeper expansion of the asymmetry in the far SOL can be observed, probably just limited by the constraint imposed by boundary conditions at the external wall. This feature, which is also observed in experimental results but not recovered by transport codes, is due to the radial transport of parallel momentum by density structures propagating outward in the SOL.

6. Summary

The new edge transport and turbulence code *TOKAM-3D* has been used to address the issue of parallel flow asymmetries in the SOL of tokamaks. The characteristics of this code allow a coherent insight on this issue without having to rely on ad-hoc hypotheses concerning the shape of potential profiles or the poloidal distribution of transport coefficients. Our results, confirm the existence of two different mechanisms susceptible to generate large amplitude parallel flows in the edge, both driven by mechanisms in which parallel fluxes are driven by parallel gradients to compensate for perpendicular transport poloidal symmetry breaking linked to curvature. On the one hand, the natural development of a potential profile generates a poloidal ExB rotation of the plasma which, along with the obstacle that constitutes the limiter, tends to accumulate

density on the outboard side of the limiter. On the other hand, turbulent transport itself exhibits a strongly ballooned distribution which leads to higher density on the LFS. Both mechanisms overlap in the SOL of tokamaks leading to good qualitative and quantitative agreement with experimental parallel flow patterns.

Thus, our results demonstrate the possibility to recover important experimental trends by adopting a fully consistent approach of the transport physics in the edge, even though deeper investigation is necessary to push further the comparison with experimental results. This may require including new physics ingredients in the model, like the impact of temperature profiles or of ionization and recycling sources.

Acknowledgements

UKAEA authors were funded jointly by the UK EPSRC and by the European Communities under the contract of Association between EURATOM and UKAEA. The views and opinions expressed herein do not necessarily reflect those of the European Commission.

References

- [1] T. Tala et al., *Plasma Phys. Control. Fusion* 49 (2007) B291.
- [2] N. Asakura, *J. Nucl. Mater.* 363–365 (2007) 41.
- [3] J.P. Gunn et al., *J. Nucl. Mater.* 363–365 (2007) 484.
- [4] G.D. Porter et al., *J. Nucl. Mater.* 313–316 (2003) 1085.
- [5] S.K. Erents et al., *Plasma Phys. Control. Fusion* 46 (2004) 1757.
- [6] R. Zagórski et al., *Plasma Phys. Control. Fusion* 49 (2007) S97.
- [7] P. Tamain et al., *J. Comput. Phys.*, accepted for publication.
- [8] P. Tamain, *Etude des Flux de Matière dans le Plasma de Bord des Tokamaks: Alimentation, Transport et Turbulence*, PhD Thesis, Université de Provence, Marseille, France, 2007.
- [9] B. Scott, *Low Frequency Fluid Drift Turbulence in Magnetized Plasmas*, IPP 5/92, 2001.